Adsorption and Reactions of NO on Clean and CO-Precovered Ir(111)

Tadahiro Fujitani,*,† Isao Nakamura,† Yukihiro Kobayashi,‡ Atsushi Takahashi,§ Masaaki Haneda,§ and Hideaki Hamada§

Research Institute for Innovation in Sustainable Chemistry, National Institute of Advanced Industrial Science and Technology (AIST), AIST Tsukuba West, 16-1 Onogawa, Tsukuba, Ibaraki 305-8569, Japan, Department of Life and Environmental Sciences, Faculty of Engineering, Chiba Institute of Technology, 2-17-1 Tsudanuma, Narashino, Chiba 275-0016, Japan, Research Institute for Innovation in Sustainable Chemistry, National Institute of Advanced Industrial Science and Technology (AIST), AIST Tsukuba Central 5, 1-1-1 Higashi, Tsukuba, Ibaraki 305-8565, Japan

Received: June 9, 2005; In Final Form: July 19, 2005

Adsorption and reactions of NO on clean and CO-precovered Ir(111) were investigated by means of X-ray photoelectron spectroscopy (XPS), high-resolution electron energy loss spectroscopy (HR-EELS), infrared reflection absorption spectroscopy (IRAS), and temperature-programmed desorption (TPD). Two NO adsorption states, indicative of fcc-hollow sites and atop sites, were present on the Ir(111) surface at saturation coverage. NO adsorbed on hollow sites dissociated to N_a and O_a at temperatures above 283 K. The dissociated N_a desorbed to form N_2 by recombination of N_a at 574 K and by a disproportionation reaction between atop-NO and N_a at 471 K. Preadsorbed CO inhibited the adsorption of NO on atop sites, whereas adsorption on hollow sites was not affected by the coexistence of CO. The adsorbed CO reacted with dissociated O_a and desorbed as CO_2 at 574 K.

1. Introduction

Selective reduction of NO in oxidizing atmospheres has recently received much attention because it has potential as a practical measure to remove NOx emitted from diesel and lean-burn engines. Many studies of various types of reductants for the selective catalytic reduction of NO have been carried out. Recently, H_2 and CO have begun to attract attention as effective reducing agents. Yokota et al.[1] reported that Pt/mordenite is active for NO reduction with H_2 in the presence of O_2 at around 423 K. They also found that Mo and Na additives widen the temperature window for the reaction. Several researchers have investigated the selective reduction of NO with H_2 over Pt- and Pd-based catalysts.[2−5] Ogura et al.[6] have reported that NO can be reduced to N_2 with CO over supported iridium catalysts such as Ir/silicalite and that the catalytic activity is not influenced by coexisting SO_2. Wang et al.[7] investigated Pt, Pd, Rh, and Ir catalysts and reported that an Ir/ZSM-5 catalyst exhibited high activity for NO reduction by CO in the presence of excess O_2. The selective catalytic reduction of NO with CO also takes place over supported metal oxide catalysts such as Cu/Al_2O_3.[8] However, comparison of the activity of various supported metallic catalysts under the identical conditions revealed that Cu/Al_2O_3 is not very active and that supported iridium catalysts are the most active for NO reduction with CO.[9] Recently, Yoshinari et al. discovered that Ir/SiO_2 and Rh/SiO_2 show marked catalytic activity for NO reduction with H_2 in the presence of O_2 and SO_2.[10,11] The Ir/SiO_2 catalyst also shows excellent activity with respect to NO reduction with CO in the presence of O_2 and SO_2.[12]

These results indicate that Ir metal is an effective catalyst for the selective reduction of NO with CO. However, the fundamental aspects of the adsorption and reaction processes on the Ir surface are not clearly understood. To develop catalysts with higher performance and durability, these processes must be understood at the molecular level. In this paper, we report on our studies of the adsorption and reactions of NO on clean and CO-precovered Ir(111) using X-ray photoelectron spectroscopy (XPS), high-resolution electron energy loss spectroscopy (HR-EELS), infrared reflection absorption spectroscopy (IRAS), and temperature-programmed desorption (TPD).

2. Experimental Section

XPS experiments were performed in an ultrahigh vacuum (UHV) apparatus composed of two chambers: a surface-analysis chamber ($<1 \times 10^{-10}$ Torr) and a preparation chamber ($<1 \times 10^{-8}$ Torr). The analysis chamber was equipped with an ion gun for Ar^+ sputtering, a photoelectron analyzer for XPS, and dosers for adjusting the NO and CO exposures. XPS spectra were measured with Mg Kα radiation. Coverage was estimated by XPS on the basis of the oxygen-buildup curve at 300 K; the oxygen saturation coverage on the Ir(111) surface is 0.5 (a coverage value (Θ) of 1 corresponds to the number of surface Ir atoms, 1.57×10^{15} atoms/cm^2).[13] The nitrogen, oxygen, and carbon coverages were determined from the N 1s/Ir $4f_{7/2}$, O 1s/Ir $4f_{7/2}$, and C 1s/Ir $4f_{7/2}$ peak area ratios, using the O 1s/Ir $4f_{7/2}$ peak area ratio obtained from the oxygen saturation coverage and the sensitivity factors for N 1s, O 1s, and C 1s.[14]

The IRAS, HR-EELS, and TPD experiments were carried out in a UHV apparatus composed of four chambers: a load-lock chamber for changing samples ($<1 \times 10^{-9}$ Torr); a preparation chamber equipped with an ion gun for Ar^+ sputtering; an analysis chamber for the HR-EELS, Auger electron spectroscopy (AES), and quadrupole mass spectroscopy equip-

* To whom correspondence should be addressed. Tel: +81-298-61-8173; fax: +81-298-61-8172; e-mail: t-fujitani@aist.go.jp.
† AIST Tsukuba West.
‡ Chiba Institute of Technology.
§ AIST Tsukuba Central.

10.1021/jp053092t CCC: $30.25
Published on Web 08/25/2005

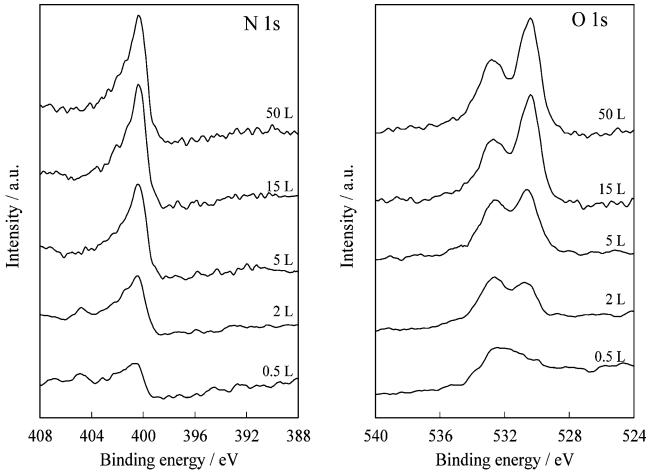

Figure 1. N 1s and O 1s XP spectra of Ir(111) after various ^{15}NO exposures at 170 K.

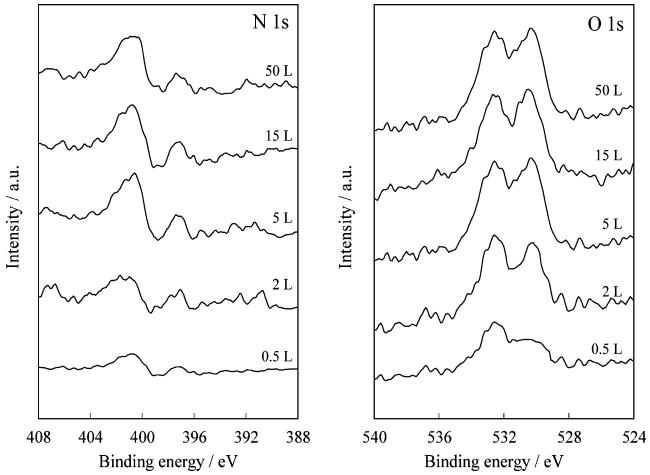

Figure 2. N 1s and O 1s XP spectra of Ir(111) heated to 310 K after various ^{15}NO exposures.

ment ($<8 \times 10^{-11}$ Torr); and a reaction chamber ($<9 \times 10^{-10}$ Torr) in which the NO and CO adsorption experiments were performed. An infrared spectrometer with a liquid nitrogen-cooled mercury−cadmium−telluride detector was situated in the reaction chamber. The spectra were recorded at a resolution of 4 cm^{-1} with 100 scans over a total measurement time of 30 s. HR-EEL spectra were measured with a double-pass cylindrical monochromator and analyzer. The typical energy resolution was 40 cm^{-1}.

The Ir(111) single-crystal disk (8-mm diameter, 1-mm thickness, 99.999% purity) was polished on only one plane. The crystal plane was accurate to within 1 degree, and the surface roughness was less than 0.03 μm. The sample was mounted using two 0.25-mm diameter tantalum wires for resistive heating. The temperature of the sample was measured with a chromel−alumel thermocouple spot-welded to the back of the crystal. The Ir surface was cleaned by repeated Ar^+ sputtering at 1000 K for 20 min, annealing at 1000 K in 3×10^{-7} Torr of oxygen for 10 min, and flashing to 1200 K in a vacuum. The cleanliness of the sample was checked by AES or XPS.

Adsorption experiments with ^{15}NO (99.9% pure) and CO (99.999% pure) were carried out at 5×10^{-9}−5×10^{-8} Torr of exposure and a sample temperature of 170−373 K. The TPD experiments were performed at a 1.0 K/s heating rate. The ^{15}NO gas was used to distinguish the N_2 desorption peak from the CO desorption peak as well as the N_2O desorption peak from the CO_2 desorption peak during TPD. We confirmed that no CO or CO_2 was desorbed from the NO-adsorbed surface, which indicates that there was no CO impurity in the NO gas.

3. Results and Discussion

3.1. Adsorption and Reaction of NO on Ir(111). Adsorption of NO on Ir(111) was investigated using XPS. In the N 1s and O 1s XPS spectra of Ir(111) measured after various NO exposures at 170 K (Figure 1), we observed the N 1s peak at 400.3 eV (which is close to the value for molecularly adsorbed NO on the surface[15]) and two O 1s peaks at 530.4 and 532.8 eV. The peak intensities of N 1s and O 1s increased with increasing NO exposure and then saturated at 15 L. From the N 1s peak area, we estimated the saturation coverage of N to be 0.46. The saturation coverages of oxygen determined from the 530.4- and 532.8-eV peaks were 0.32 and 0.15 (total oxygen coverage, 0.47). The coverage ratios of O and N were almost equal, which indicates that the O 1s peaks at 530.4 and 532.8 eV were due to molecularly adsorbed NO on the surface. These

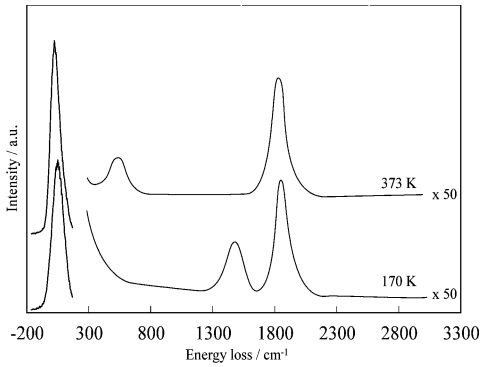

Figure 3. HR-EEL spectra of Ir(111) after ^{15}NO exposure (10 L) at 170 and 373 K.

results clearly indicate that two adsorbed NO species were present on the Ir(111) surface.

Zhu et al. also observed two O 1s peaks for adsorbed NO on Pt(111) at 110 K: a peak at 530−530.6 eV, assigned to NO adsorbed on hollow sites, and a peak at 532.0 eV, assigned to NO adsorbed on atop sites.[16] On the basis of their results, we assigned that the peaks we observed at 530.4 and 532.8 eV to NO adsorbed on hollow sites (hollow-NO) and atop sites (atop-NO) of Ir(111), respectively. Thus, the ratio of hollow-NO to atop-NO was 2.1, and the NO saturation coverage on the Ir-(111) surface was approximately 0.5 at 170 K.

The Ir crystal containing the NO molecules adsorbed at 170 K was heated to 310 K, and the N 1s and O 1s XPS spectra of Ir(111) were measured after various NO exposures (Figure 2). In addition to the N 1s peak at 400.3 eV (ascribed to molecularly adsorbed NO), we observed a new peak (at 397.4 eV), corresponding to atomic nitrogen,[15] which indicates that the NO adsorbed on the Ir(111) had dissociated to atomic nitrogen and oxygen at around 310 K. In the O 1s spectra, the intensity of the peak at 532.8 eV because of the atop-NO was not altered by heating to 310 K, indicating that the atop-NO was stable on Ir(111) at this temperature. In contrast, the intensity of the peak at 530.4 eV decreased by heating to 310 K. From the results of N 1s spectra, the peak at 530.4 eV could be due to the atomic oxygen from the dissociation of hollow-NO.

The adsorption state of NO on the Ir(111) surface was also investigated using HR-EELS. In the HR-EEL spectra after saturation of the surface with NO (exposure 10 L) at 170 K and annealing to 373 K (Figure 3), peaks at 1470 and 1856 cm^{-1} were observed at the surface temperature of 170 K.

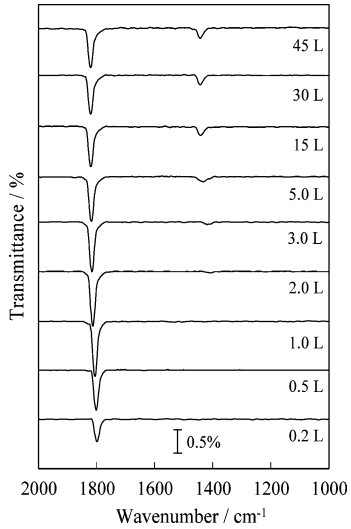

Figure 4. IRA spectra of NO adsorbed on Ir(111) after ^{15}NO exposure at 0.2−45 L at 263 K.

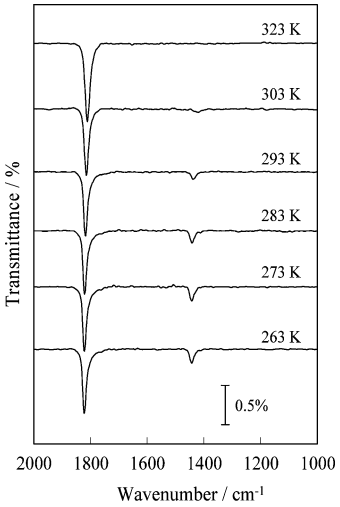

Figure 5. IRA spectra of Ir(111) after ^{15}NO exposure at various temperatures.

Matsumoto et al. studied[17] the structure of NO on a Pt(111) surface using scanning tunneling microscopy and HR-EELS and assigned the EELS peaks they observed at 1444, 1508, and 1715 cm^{-1} on the NO-saturated surface to NO molecules adsorbed on fcc-hollow, hcp-hollow, and atop sites, respectively. Therefore, we assigned the peaks we observed at 1470 and 1856 cm^{-1} on the Ir(111) surface to NO adsorbed on fcc-hollow and atop sites, respectively. Cornish et al. also studied the adsorption of NO on Ir(111) by EELS,[18] and they observed a predominant peak at 1860 cm^{-1} at low NO coverage and peaks at 1480 and 1550 cm^{-1}, as well as at 1860 cm^{-1}, at high NO coverage. Their results indicate that NO selectively adsorbed at atop sites at low NO coverage and that NO adsorbed at hollow sites at higher NO coverage. Using a slab model, Aizawa et al.[19] calculated the frequencies of the N−O stretching modes of atop, fcc-hollow, and hcp-hollow NO/Pt(111) species at a coverage of 0.75 to be 1708, 1463, and 1540 cm^{-1}, respectively. Their results were in good agreement with those of Cornish et al.[18] At a coverage of 0.5, they indicated[19] that the N−O stretching modes of atop and fcc-hollow species have frequencies of 1703 and 1447 cm^{-1}, respectively.

Because the NO coverage on the Ir(111) surface was about 0.5 in our study, we assigned the peak at 1470 cm^{-1} in Figure 3 to NO adsorbed on fcc-hollow sites. We observed no hcp-hollow NO at a NO coverage of 0.5. The peak at 1470 cm^{-1} corresponding to NO adsorbed on hollow sites disappeared completely after the surface was annealed at 373 K, and a new peak was observed at 524 cm^{-1}. This peak was due to atomic oxygen, considering that the adsorbed NO on the hollow site dissociated to N_a and O_a below 373 K. We observed no change in the peak intensity for NO adsorbed on atop sites.

We also investigated the adsorption state of NO on the Ir(111) surface using IRAS. In the IRA spectra of adsorbed NO on Ir(111) exposed to NO gas at 0.2−45 L at 263 K (Figure 4), the peaks due to NO adsorbed on hollow and atop sites were observed at 1400−1444 and 1799−1820 cm^{-1}, respectively. Only the peak for NO adsorbed on atop sites was observed at the initial state of exposure to NO, which indicates that the NO was selectively adsorbed on atop sites at low NO coverage. The intensity of the peak for NO adsorbed on atop sites increased with increasing NO exposure up to 2 L and then slightly decreased. The intensity of the peak for atop NO was constant at exposures above 15 L. In contrast, NO began to adsorb on hollow sites at exposures above 2 L. The intensity of the hollow-NO peak increased with increasing NO exposure up to 15 L and then became saturated. As can be seen in Figure 4, the peak intensity of the hollow-NO species was much smaller than that of the atop-NO species at saturation, although the hollow-NO coverage was twice that of the atop-NO species. Aizawa et al. have reported normal-model frequencies and peak intensities of NO/Pt(111) at various coverages,[19] and they found that the N−O stretching peak intensity of fcc-hollow species greatly decreased in the presence of coexisting atop species. This effect is not due to the well-known intensity-transfer effect derived from dynamic dipole−dipole coupling but to a change in the electronic state of the adsorption system caused by the coexistence of the atop species. The calculated data[19] are in good agreement with our experimental results. In the IRA spectra we measured after saturation of the surface with NO at 263 K and annealing in a vacuum to 323 K (Figure 5), the peak intensities for NO adsorbed on atop sites (1811−1820 cm^{-1}) remained constant up to 323 K. In contrast, the intensity of the peak for NO adsorbed on hollow sites was reduced at 283 K, and the peak completely disappeared at 323 K, which indicates that NO adsorbed on hollow sites dissociated above 283 K. This result was consistent with our XPS and EELS results.

We investigated the thermal reactivity of ^{15}NO on the Ir(111) surface using TPD. In the TPD spectra for ^{15}NO and $^{15}N_2$ after saturation of the surface with NO at 263 K, we did not observe any desorption peaks for N_2O and O_2 on the Ir(111) surface, which indicates that atomic oxygen dissociated from NO remained on the surface at temperatures below 900 K (Figure 6). Two desorption peaks for ^{15}NO were observed, at 393 and 455 K. In light of the XPS and EELS results, which indicate that only atop-NO species existed on the Ir surface after annealing to 373 K, we assigned the peaks at 393 and 455 K to desorption of ^{15}NO adsorbed on hollow and atop sites, respectively. Simultaneously with ^{15}NO desorption, the $^{15}N_2$ desorption peaks were observed at 471 and 574 K.

The mechanism of the decomposition of NO on Rh(111) was reported by Root and co-workers,[20] who observed the two desorption peaks of N_2 at 473 and 560 K at saturation coverage of NO. They suggested that the N_2 desorption peak at 473 K could be attributed to a disproportionation reaction, $NO_a + N_a \rightarrow N_{2g} + O_a$, and they attributed the peak at 560 K to recombination of N_a. On the basis of their results, we assigned the $^{15}N_2$ peaks we observed at 471 and 574 K to a disproportionation reaction between atop-NO and N_a dissociated from hollow-NO and to the recombination of N_a, respectively.

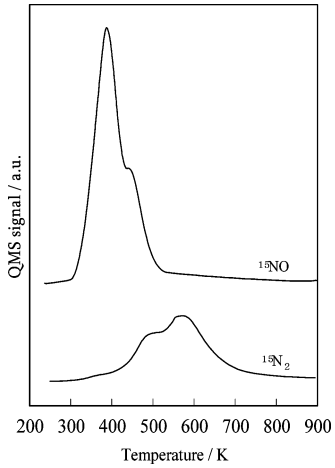

Figure 6. TPD spectra of ^{15}NO adsorbed on Ir(111). Adsorption temperature, 263 K; exposure, 45 L; heating rate, 1 K/s.

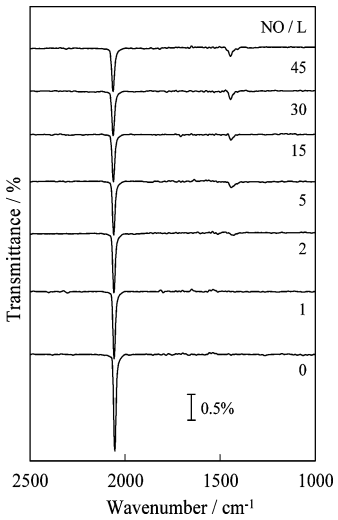

Figure 7. IRA spectra of ^{15}NO on Ir(111) at various exposure levels at 273 K after preadsorption of CO at saturation ($\Theta_{CO} = 0.33$).

3.2. Adsorption and Reaction of NO on CO−Precovered Ir(111). We investigated the adsorption of NO on a CO-precovered Ir(111) surface by means of IRAS (Figure 7). In the IRA spectra at various NO exposures at 273 K on Ir(111) with CO preadsorbed at saturation coverage ($\Theta = 0.33$), we observed the peak due to the C−O stretching mode at 2060 cm^{-1} for the CO-precovered surfaces.[21,22] The intensity of the adsorbed-CO peak decreased with increasing NO exposure up to 15 L and then remained constant. The peak that corresponded to NO adsorbed on hollow sites was observed at 1440 cm^{-1} after NO exposure, and the peak intensity was constant at exposures above 15 L. No peak due to NO adsorbed on atop sites (1820 cm^{-1}) was observed on the CO-precovered Ir surface, which indicates that the CO inhibited NO adsorption only on atop sites.

We also investigated the adsorption of NO on a CO-precovered ($\Theta_{CO} = 0.33$) Ir(111) surface using XPS (Figure 8). We observed the O 1s peak due to the adsorbed CO on Ir surface at 532.4 eV for the CO-precovered surface, which is close to the peak for NO adsorbed on atop site. The O 1s peak at 530.5 eV corresponding to NO adsorbed on hollow site appeared with NO exposure. The coverage of NO adsorbed on hollow site increased with increasing NO exposure up to 15 L and then was constant. The NO coverage at 15 L was estimated to be 0.31, which was the same as the coverage for the clean

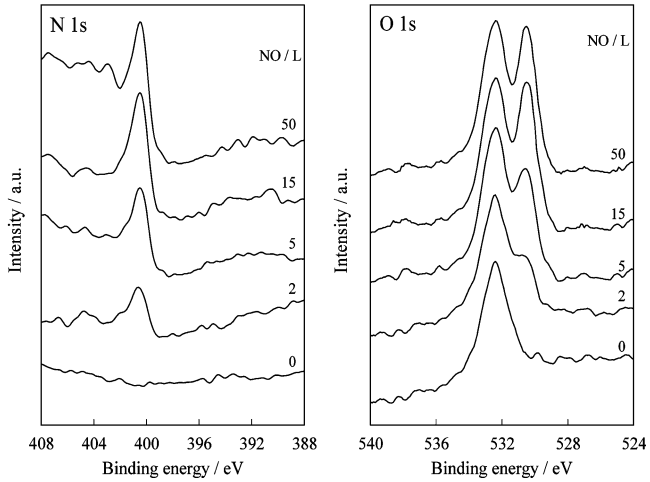

Figure 8. N 1s and O 1s XP spectra of ^{15}NO on Ir(111) at various exposure levels at 273 K after preadsorption of CO at saturation ($\Theta_{CO} = 0.33$).

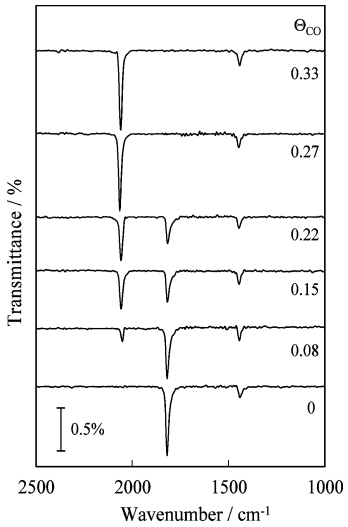

Figure 9. IRA spectra of ^{15}NO on Ir(111) at 45 L at 273 K after preadsorption of CO at various coverages.

Ir(111) surface. In contrast, the intensity of O 1s peak at 532.4 eV was constant during NO exposure, indicating that the coverage of preadsorbed CO was not influenced by exposure of NO. Therefore, we considered that the decrease in the IR peak intensity of adsorbed CO by the NO adsorption is not due to the reduction of the CO concentration but is considered to be due to the change of the adsorption geometry of CO. In the N 1s spectra, we observed the peak at 400.4 eV to be due to molecularly adsorbed NO on the surface. The coverage ratios estimated from O 1s peak at 530.5 eV and N 1s peak at 400.4 eV were almost equal, suggesting that NO adsorbed on only hollow site on a CO-precovered surface. Thus, we propose that the atop sites on Ir(111) were occupied by adsorbed CO whereas the hollow sites were vacant in the presence of CO.

We used IRAS to obtain further details regarding the adsorption state of NO on Ir(111) with CO preadsorbed at a coverage below 0.33 (Figure 9). In the IRA spectra of NO exposed at 273 K at 45 L on the Ir(111) surface precovered at various CO coverages, the peak intensities of NO adsorbed on atop sites decreased with increasing CO coverage, and the peaks disappeared after the preadsorbed CO coverage reached approximately 0.27. In contrast, we observed no change in the peak for NO adsorbed on hollow sites, even when preadsorbed CO was present. These results clearly demonstrate that pre-

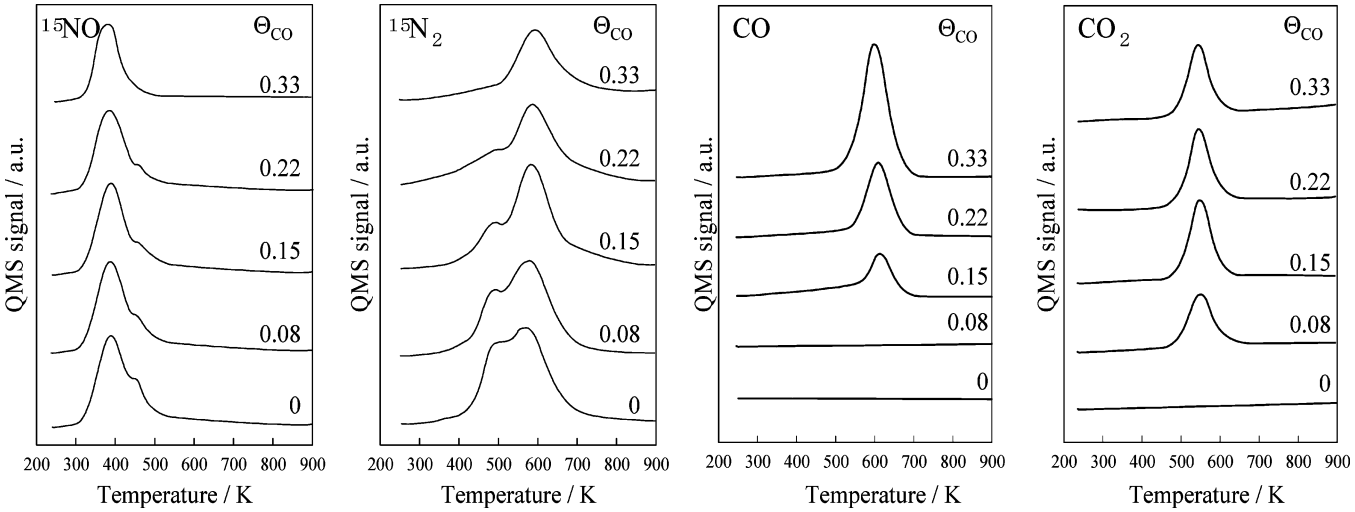

Figure 10. TPD spectra of ^{15}NO adsorbed on Ir(111) after preadsorption of CO at various coverages. NO adsorption temperature, 273 K; exposure, 45 L; heating rate, 1 K/s.

adsorbed CO, which selectively adsorbed on atop sites of Ir(111), inhibited adsorption of atop-NO, whereas the adsorption of NO on hollow sites was not affected by the presence of adsorbed CO.

The thermal reaction between CO and ^{15}NO on Ir(111) was examined by TPD. In the ^{15}NO spectra (Figure 10), the peaks that appeared at around 460 K decreased as the amount of preadsorbed CO increased, and the peaks disappeared at a CO coverage of 0.33. However, the ^{15}NO desorption peak at 400 K remained constant regardless of the coverage of preadsorbed CO. The results shown in Figure 9 indicate that NO adsorbed on atop sites decreased with increasing CO precoverage, but hollow-site NO was present on Ir(111) at any coverage of preadsorbed CO. Thus, the desorption peaks at 400 and 460 K were due to desorption of NO adsorbed on hollow and atop sites, respectively.

Similar changes in the TPD spectra were observed for the desorption of $^{15}N_2$. The peaks at 470 K decreased with increasing CO precoverage, whereas the peaks at 570 K remained constant regardless of CO coverage. Because atop-NO species were reduced by the presence of CO, the $^{15}N_2$ peak due to the disproportionation reaction between atop-NO and N_a dissociated from hollow-NO disappeared with increasing CO exposure. This result clearly indicates that the $^{15}N_2$ peaks at 471 and 574 K were due to a disproportionation reaction between atop-NO and N_a dissociated from hollow-NO and to the recombination of N_a, respectively. A CO desorption peak was observed at around 600 K, and this peak increased with increasing CO exposure. After N_2 desorption, the CO_2 formation peak was observed at 574 K, a temperature that was lower than the CO desorption temperature (600 K). Thus, CO_2 was produced by the reaction of adsorbed CO and atomic O produced by dissociation of NO adsorbed in the hollow sites.

4. Conclusions

We studied the adsorption and reactions of NO on clean and CO-precovered Ir(111) by using XPS, HR-EELS, IRAS, and TPD. XPS results indicate the presence of two NO adsorption states, indicative of fcc-hollow sites and atop sites, on the Ir(111) surface at 170 K. Two NO adsorption states were also observed by IRAS and HR-EELS. NO was selectively adsorbed on atop sites at low NO coverage and then began to be adsorbed on hollow sites as NO coverage increased. The saturation coverage of NO was estimated to be 0.46, and the ratio of hollow-NO to atop-NO was determined to be approximately 2. NO adsorbed on hollow sites dissociated to N_a and O_a above 283 K. The dissociated N_a desorbed to produce N_2 at the two temperatures by recombination of N_a at 574 K and by a disproportionation reaction between atop-NO and N_a at 471 K.

Only NO adsorbed on hollow sites was observed on CO-precovered Ir(111), which indicates that the CO selectively adsorbed on atop sites and inhibited the adsorption of NO on atop sites. TPD results showed the formation of CO_2 after N_2 desorption, which indicates that the adsorbed CO reacted with O_a dissociated from hollow-NO.

Acknowledgment. This work was supported by the Japan Society for the Promotion of Science (JSPS-KAKENHI 17350079).

References and Notes

(1) Yokota, K.; Fukui, M.; Tanaka, T. *Appl. Surf. Sci.* **1997**, *121−122*, 273.
(2) Burch, R.; Shestov, A. A.; Sullivan, J. A. *J. Catal.* **1999**, *188*, 69.
(3) Ueda, A.; Nakao, T.; Azuma, M.; Kobayashi, T. *Catal. Today* **1998**, *45*, 135.
(4) Macleod, N.; Lambert, R. M. *Chem. Commun.* **2003**, 1300.
(5) Machida, M.; Ikeda, S.; Kurogi, D.; Kijima, T. *Appl. Catal. A* **2001**, *35*, 107.
(6) Ogura, M.; Kawamura, A.; Matsukata, M.; Kikuchi, E. *Chem. Lett.* **2000**, 146.
(7) Wang, A.; Ma, L.; Cong, Y.; Zhang, T.; Liang, D. *Appl. Catal. B* **2003**, *40*, 319.
(8) Yamamoto, T.; Tanaka, T.; Kuma, R.; Suzuki, S.; Amano, F.; Shimooka, Y.; Kohno, Y.; Funabiki, T.; Yoshida, S. *Phys. Chem. Chem. Phys.* **2002**, *4*, 2449.
(9) Shimokawabe, M.; Umeda, N. *Chem. Lett.* **2004**, *33*, 534.
(10) Yoshinari, T.; Sato, K.; Haneda, M.; Kintaichi, Y.; Hamada, H. *Catal. Commun.* **2001**, *2*, 155.
(11) Yoshinari, T.; Sato, K.; Haneda, M.; Kintaichi, Y.; Hamada, H. *Appl. Catal. B* **2003**, *41*, 157.
(12) Haneda, M.; Pusparatu; Kintaichi, Y.; Nakamura, I.; Sasaki, M.; Fujitani, T.; Hamada, H. *J. Catal.* **2005**, *229*, 197.
(13) Marinova, Ts.; Kostov, K. L. *Surf. Sci.* **1987**, *185*, 203.
(14) *Handbook of X-ray Photoelectron Spectroscopy*; Muilenberg, J. E., Ed.; Perkin-Elmer: Eden Prairie, MN, 1979.
(15) Lizzit, S.; Baraldi, A.; Cocco, D.; Comelli, G.; Paolucci, G.; Rosei, R.; Kiskinova, M. *Surf. Sci.* **1998**, *228*, 410.
(16) Zhu, J. F.; Kinne, M.; Fuhrmann, T.; Denecke, R.; Steinrück, H.-P. *Surf. Sci*. **2003**, *529*, 384.
(17) Matsumoto, M.; Fukutani, K.; Okano, T.; Miyake, K.; Shigekawa, H.; Kato, H.; Okuyama, H.; Kawai, M. *Surf. Sci.* **2000**, *454*, 101.
(18) Cornish, J. C. L.; Avery, N. R. *Surf. Sci.* **1990**, *235*, 209.
(19) Aizawa, H.; Morikawa, Y.; Tsuneyuki, S.; Fukutani, K.; Ohno, T. *Surf. Sci.* **2002**, *514*, 394.
(20) Root, T. W.; Schmidt, L. D. *Surf Sci.* **1983**, *134*, 30.
(21) Marinova, Ts. S.; Chakarov, D. V. *Surf. Sci.* **1987**, *192*, 275.
(22) Chakarov, D. V.; Marinova, Ts. *Surf. Sci.* **1990**, *227*, 297.